EVOLUTION OF GAS PERMEABILITY FOR CONCRETE MATERIALS UNDER AND AFTER UNI-AXIAL LOADING

Chunsheng Zhou [1, 2, *], Wei Chen [3] and Wei Wang [1, 2]
[1] Key Lab of Structures Dynamic Behaviour and Control (Harbin Institute of Technology), Ministry of Education, Heilongjiang, Harbin 150090, China. *Email: zhouchunsheng.HIT@gmail.com
[2] School of Civil Engineering, Harbin Institute of Technology, Heilongjiang, Harbin 150090, China.
[3] Ecole Centrale de Lille, Laboratoire de Mecanique de Lille, BP 48 F-59650 Villeneuve d'Ascq, France.

ABSTRACT

Under life-cycle service conditions, gas permeability which is usually employed to indicate the durability performance of concrete materials will be changed along with the evolution of microstructure under or after loading. This paper reports an extensive experimental research on the influence of loading condition on the evolution of gas permeability. A cyclic loading scheme under displacement control, which is employed to accelerate the evolution of its microstructure and model the loading condition under real service, is applied on cylinder specimens ϕ37×74mm dried to constant weight at 60°C. Both axial and lateral strains in the whole loading test are recorded by strain gauge to characterize the change of microstructure macroscopically. At the same time, gas permeability measurement is carried out by a well-designed tri-axial permeater at various loading levels in the planned loading history. The relationship between intrinsic gas permeability, Klinkenberg coefficient and residual strains discussed. It is found that intrinsic gas permeability will become great if the uni-axial loading level is beyond about 70% ultimate strength. Moreover, both the klinkenberg coefficient and intrinsic gas permeability are badly linked with elastic and plastic strains. However, the relationship between the Klinkenberg coefficient and intrinsic gas permeability can be approximated by a semi-empirical law, no matter under or after loading.

KEYWORDS

Concrete, intrinsic gas permeability, klinkenberg coefficient, residual strain.

INTRODUCTION

The durability of structural concrete is degraded due to the ingression of external aggressive agents such as water, carbon dioxide as well as chloride ion etc. (Cerny 2002). Mass transport properties play the central role in the analysis of durability performance thus the service life (AFGC 2007). Moreover, in some other fields including geotechnical, petroleum, hydrogeology and waste management, the analysis of mass transport in fractured porous materials is of great interest (Reinhardt 1997). Especially, the prediction of waste transport in nuclear waste depository should be paid enough attention due to its significant importance and possible negative influence (Verdier *et al*. 2002). It should be emphasized that, structural concrete material is always subjected to mechanical action, which will make the mass transport properties of porous medium changed greatly due to the possible generation and opening of cracks. The influence of mechanical action or possible cracking should be taken into account when quantitatively predicting the detailed mass transport process.

As a quasi-brittle porous material, structural concrete is vulnerable to micro-cracking under the action of environmental and mechanical actions (Mehta and Monteiro 2006). The ingression of external aggressive agents including liquid, gas and ions will remarkably benefit from this factor. Vast researchers have made great efforts to study the influence of mechanical action on the transport of liquid, gas as well as ion species (Hoseini *et al*. 2009; Zhou *et al*. 2012a, b). To understand the detailed influencing mechanism of mechanical action on mass transport, inert gas permeability is paid more attention due to the possible physical and chemical inter-actions between cracking cementitious materials and liquid with or without interested ions, which may introduce some other factors rather than pure mechanical action (Loosveldt *et al*. 2002). Moreover, in contrast to liquid permeability to water or alcohol, gas permeability is more sensitive to the number, size, orientation, opening as well as connectivity of cracks, which will facilitate the distinguish of even minor influence of cracking from the obvious scatter of concrete materials. Besides, it is also more convenient and less time-consuming to measure gas permeability since inert gas flow can quickly reach stable state even in dense concrete material.

In this paper, the evolution of gas permeability for three structural concrete materials is measured and discussed before, under and after mechanical loading. In Section 2, the preparation of materials and specimen as well as

following experimental procedures are introduced. The measured gas permeability are further given and discussed with respect to stress level and strain level in Section 3 . Finally, the concluding remarks are provided in Section 4.

EXPERIMENTS

Function Materials and specimen

To experimentally investigate the gas permeability of concrete materials under and after loading, three kinds of structural concrete materials C39, C29 and C19 with various water to cement ratios 0.39, 0.29 and 0.19 were prepared with CEM V/A. The mix proportioning of these cement-based materials used in nuclear waste storage application as candidates are detailed in Table 1. Several small beams of size 140×140×560mm were made for each concrete. At the age of 24h, these beams are demoulded and then cured in water until the age of 90 days. After curing, 5 small cylinders of the identical size ϕ37×74mm, whose diameter is about three times of maximum size of gravel, were drilled from small beams. Only the central part of the cored cylinders are cut out to obtain the target cylinder of 74mm height. The two circular end faces of each cylinder is further processed to be flat and parallel to each other to facilitate the later mechanical loading and gas permeability measurement.

Table 1 Mix proportioning and basic properties of three concrete materials

Proportioning	C39	C29	C19
Sand (Limestone, 0-5mm, kg/m^3)	729	809	729
Gravel (Limestone, 5-12mm, kg/m^3)	864	958	864
Cement (CEM V/A, 42.5N, kg/m^3)	393	436	393
Superplasticizer (Glenium 27, kg/m^3)	10.0	11.2	10.0
Water (kg/m^3)	153.8	126.9	75.2
Effective water to cement ratio (-)	0.39	0.29	0.19
Ultimate strength (3 months, MPa)	55	67	71
Maximum axial strain (με)	1850	1780	1870
Capillary porosity (%)	13.2	9.4	7.8
Elastic modulus (GPa)	33.6	43.3	43.4
Poisson's ratio (-)	0.224	0.266	0.259

After preparing 5 cylinders for each concrete materials, 3 of them are tested to obtain their elastic modulus, Poisson's ratio, ultimate strength as well as maximum axial strain. In uni-axial compression, three cycles of compression up to about 30% ultimate strength were first carried out to measure elastic modulus and Poisson's ratio. After that, cylinder specimen are further uni-axially compressed until failure to get ultimate strength and maximum axial strain. The average ultimate strength of concrete material C39, C29 and C19 is 55MPa, 67MPa and 71MPa, respectively. Due to the obvious high water to cement ratio, the strength and elastic modulus for concrete C39 is obviously lower than other two concretes. Moreover, although the water to cement ratio for concrete C29 is larger than C19, there is no remarkable difference about ultimate strength and elastic modulus between them.

Another 2 cylinders were oven-dried to constant mass under constant temperature of 60°C. The mass of each specimen is monitored every 7 days. If the relative difference between two successive measurement are smaller then 0.1%, constant mass is thought to be reached and concrete specimen is totally dried. The capillary porosity is also deduced from the mass difference of saturated and totally dried specimens, as list in Table 2.

Gas permeability measurement

Generally, permeability is understood as a transport properties characterizing the fluid bulk flow within a porous medium under pressure gradient. The flowing velocity q (LT^{-1}) is quantitatively described as follows (Reinhardt 1997),

$$q = -\frac{k}{\eta}\nabla P \tag{1}$$

in which η (Pa·s), P (Pa) and k (m^2) denotes dynamic viscosity, pressure and permeability, respectively. Theoretically, permeability k is independent on the type of penetrating fluid (Reinhardt 1997). However, due to the possible complex physical and chemical interactions between flowing fluid and porous skeleton with high specific surface, the permeability to water, alcohol and inert gas are remarkably different for cementitious materials (Loosveldt *et al*. 2002;Wang *et al*. 2014). Considering from the faced practical difficulty for experimental measurement, permeability to gas is widely adopted to characterize the mass transport properties

thus the durability performance for cementitious materials. It is well-known that gas is a kind of fluid with high compressibility, if ideal gas is assumed, then the apparent gas permeability k_A (m^2) can be calculated by (Scheidegger 1974),

$$k_A = -\frac{Q}{A}\frac{2\eta L P_{atm}}{P_i^2 - P_{atm}^2} \tag{2}$$

Where Q is the volume flow velocity of gas (m^3/s), A is cross-sectional area (m^2), L is thickness of sample (m) and P_i, P_{atm} (Pa) denotes applied inlet and outlet (atmospheric) pressure, respectively. However, the apparent permeability is dependent on the applied pressure due to the gas slippage effect on small pore walls, which is known as "Klinkenberg effect"' (Klinkenberg 1941). Taking slip flow mode and viscous flow mode into account, the actual flow of gas in tight porous media can be quantitatively described as (Klinkenberg 1941),

$$k_A = k_V\left(1+\frac{\beta}{P_m}\right), P_m = \frac{P_i + P_{atm}}{2} \tag{3}$$

in which k_V, β and P_m is the intrinsic gas permeability, Klinkenberg coefficient and average pressure, respectively. Physically, Klinkenberg coefficient β depends on the pore structure of the medium and temperature for a given gas and can be further expressed as (Klinkenberg 1941; Civan 2010)

$$\beta = \frac{c\kappa T}{\sqrt{2}\pi r^3} \tag{4}$$

where r is mean pore radius (m), κ is Boltzmann's constant (J/K), T is temperature (K), c is constant. It is experimentally verified that slippage factor β varies linearly with absolute temperature (Wei *et al*. 1986). Klinkenberg effect is significant with higher coefficient in any situation where the mean free path of gas molecular in porous medium approaches the dimension of pore or micro-cracking. Moreover, β is directly linked to the average pore size in certain sense, i.e., β increases if the mean pore size decreases.

From the above Equation (3), intrinsic gas permeability k_V can be linearly regressed from several apparent permeability k_A, which can be calculated from gas flow velocity under several different inlet pressures P_i. Herein, the gas permeability is tested on totally dried cylinder specimen of size ϕ37×74mm under and after uni-axial loading by steady state method. Thanks to the kind help from Prof. Fredric Skoczylas, a carefully designed permeater highly developed in Ecole Centrale de Lille is adopted, which has been extensively described in references (Davy *et al*. 2007; Benachour *et al*. 2008). Through a tri-axial confining cell providing hydrostatic loading on the circular face of cylindrical samples to keep it air-tight, nitrogen gas is forced to flow within the tested concrete samples under three different inlet pressures while keep the outlet pressure constant as atmosphere pressure. The regulated injection pressure and the corresponding gas flow velocity are continuously monitored every 10 minutes. If the relative difference of gas flow velocity under the same injection pressure is less than 2%, steady state flow is though to be reached. Correspondingly, the apparent permeability can be further evaluated from the steady gas flow velocity and injection pressure through Equation (2). More specifically, in this experimental research work, the hydrostatic pressure is regulated to be almost a constant 3MPa, while the injection pressures are selected as about 10, 15 and 20 Bar. After obtaining the stable velocity under different injection pressure, the apparent permeability thus intrinsic permeability is further evaluated from Equation (3). Actually, it takes about 40 minutes to reach the assumed steady flowing state for each specimen under every injection pressure. Then, one measurement of intrinsic gas permeability and Klinkenberg coefficient costs about 120 minutes.

Uni-axial loading history

To study the gas permeability of concrete materials under and after loading, an axial loading history is carefully designed to apply on each cylinder specimen through the highly developed permeater. Considering the gas permeability of concrete specimen is obviously determined by its pore and cracking structure macro-scopically relating to its strain and displacement, compressive loading is applied uni-axially on the cylinder specimen using Toni Expert machine under displacement control (0.05mm/min) rather than stress control to facilitate the gas permeability testing under the identical compressive state. To ensure the assumed uni-axial compression, the two circular surfaces of each sample is carefully polished to be flat and parallel to each other. For each specimen, the gas permeability is first measured before loading. After that, three cycles with maximum stress of about 30% ultimate strength are applied to eliminate the possible irreversible strain. Then, the specimen is subjected to a cyclic loading history, as shown in Figure 1. First cycle is conducted with the maximum stress about 50% of its strength and keep it constant to allow gas permeability testing under displacement control; then the stress is unloaded to about 5MPa constant to allow gas permeability testing too. 5 more cycles are further carried out with increasing stress ratio about 60%, 70%, 80%, 90% and 95% but constant lower stress about 5MPa. After absolutely unloading, the gas permeability is also measured.

In testing, the axial strain ε_{11} and lateral strain ε_{33} is monitored by 2 strain gauges of length 20mm, respectively. All 4 strain gauges are laid every 90° on the middle portion. The adopted permeater is specially designed to allow uni-axial compression, strain monitoring as well as gas permeability measurement at the same time. Typical stress-strain relationship for specimen C19-1 is shown in Figure 1. Since one measurement of intrinsic gas permeability and Klinkenberg coefficient takes about 120 minutes, the required time to finish the testing for one specimen with 14 measurements of gas permeability is about 28 hours. It costs about 21 work days to finish all the planned experimental testing for all 6 cylinder specimens. The measured axial and lateral strains, deduced intrinsic gas permeability and Klinkenberg coefficients are all listed in the Table 2.

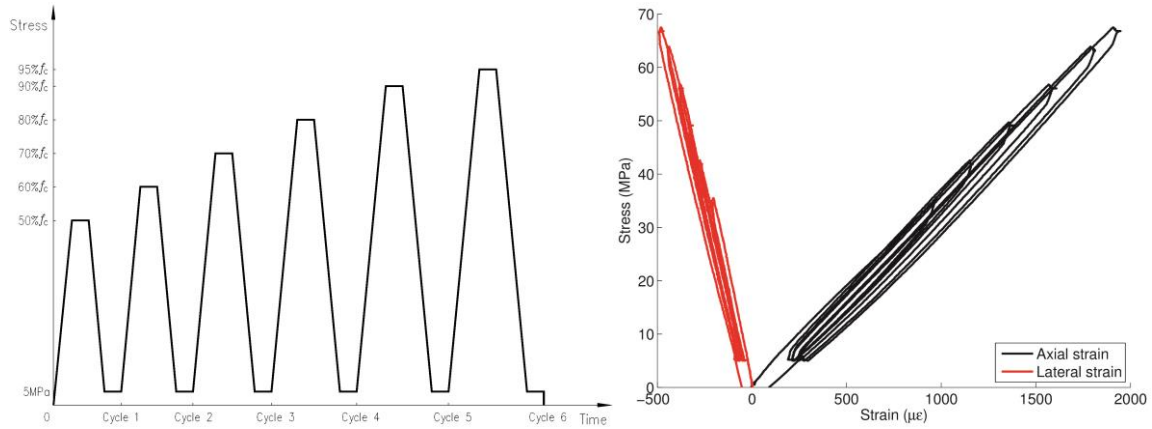

Figure 1 Designed loading history and typical stress-strain curve for specimen C19-1.

EVOLUTION OF GAS PERMEABILITY

Concrete is by nature a quasi-brittle porous material vulnerable to cracking. Generally, micro-cracking will nuclear and develop for material under loading beyond 30\% of ultimate strength. It is the micro-cracking and pore spaces where gas will flow through under pressure gradient. Along with the action of loading beyond the elastic limit, plastic strain will accumulate and the micro-structure of cracking and pores evolve. Furthermore, when damaged concrete material is subjected to loading, the compaction or opening state of micro-cracking and pores will be different from each other, which makes the gas permeability evolve. In another words, the gas permeability of micro-cracked concrete material will be changed with the current loading condition and accumulated plastic strain after loading. Herein, the evolution of gas permeability will be analyzed from these two aspects.

Gas permeability under loading

(1) Intrinsic gas permeability

For the three structural concrete materials concerned herein, the intrinsic gas permeability as well as corresponding Klinkenberg coefficient have been determined from gas permeability testing, which are listed in Table 2. To consistently analyze the relationship between gas permeability and stress / strain ratio for different materials, the relative intrinsic gas permeability k_r and stress ratio σ_r, strain ratio ε_r are introduced and defined as,

$$k_r = k_V^c / k_V^0, \sigma_r = \sigma_c / \sigma_m, \varepsilon_r = \varepsilon_c / \varepsilon_m \quad (5)$$

where k^c_V, σ_c and ε_c is the intrinsic gas permeability under compression, compressive stress and strain, respectively; k^0_V, σ_m and ε_m is the intrinsic gas permeability before loading, maximum stress and strain, respectively. The evolution of intrinsic gas permeability is plotted against the applied axial stress and accumulated strain (including elastic and plastic strains), as shown in Figure 2.

The first observation from Figure 2 is that the relationship between intrinsic permeability and stress, strain is of much scatter. For specimen C19-1, even the first loading level is just 50% of its ultimate strength, the intrinsic gas permeability is obviously larger than the situation before loading, indicating that there are remarkable micro-cracks developed before loading to half of its ultimate strength. When the stress level increases up to about 70% of its ultimate strength, the intrinsic gas permeability tends to be smaller even though more micro-cracks have been introduced by loading. It is easily inferred that there is obvious compaction or consolidation of pores and micro-cracks, which conquer the contribution of newly developed micro-cracks. Beyond 70% of its ultimate strength, the intrinsic gas permeability begins to increase quickly along with the rising of uni-axial loading stress, which attribute to the development of new micro-cracks and their opening.

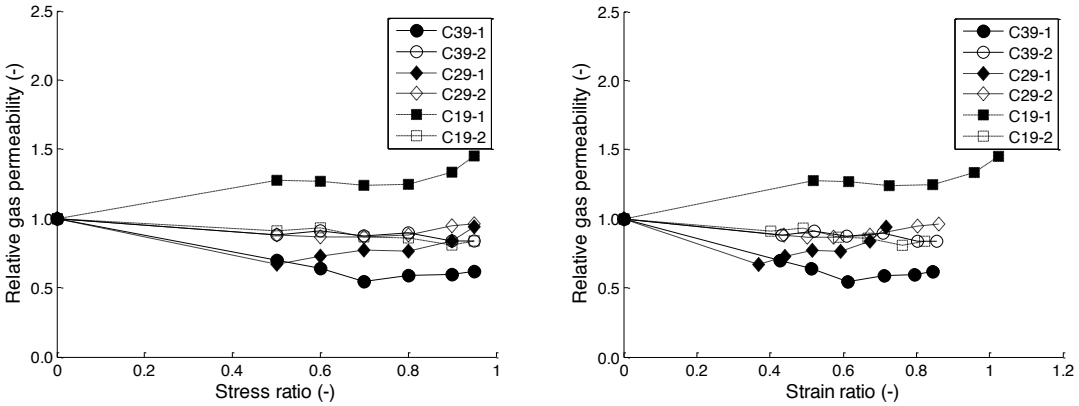

Figure 2 The evolution of relative gas permeability with stress ratio (Left) and strain ratio (Right).

Table 2 Measured strains and corresponding gas permeability of three concrete before, under and after loading

Specimen	Property	Before loading	Cycle 1		Cycle 2		Cycle 3		Cycle 4		Cycle 5		Cycle 6		After loading
			50%	5MPa	50%	5MPa	50%	5MPa	50%	5MPa	50%	5MPa	50%	5MPa	
C39-1	ε_{11} (με)	0	789.4	262.4	951.4	295.6	1133.0	359.1	1316.8	356.5	1472.7	385.7	1562.4	405.8	143.4
	ε_{33} (με)	0	-141.6	-34.9	-180.2	-33.0	-216.0	-45.1	-267.4	-44.1	-301.7	-42.1	-324.5	-44.3	-9.4
	k_v (E-18m^2)	6.279	4.367	5.130	4.019	4.908	3.428	4.881	3.694	4.790	3.754	4.948	3.897	4.753	5.725
	β (Bar)	2.426	3.843	3.423	4.074	3.340	4.965	2.822	3.586	3.011	3.477	2.942	3.324	3.570	2.665
C39-2	ε_{11} (με)	0	798.8	198.9	962.2	202.0	1129.6	226.9	1311.4	254.1	1487.8	281.6	1582.2	299.5	100.7
	ε_{33} (με)	0	-209.4	-49.8	-256.7	-64.1	-307.2	-68.3	-362.2	-67.8	-414.4	-79.9	-457.9	-87.0	-37.2
	k_v (E-18m^2)	2.630	2.316	3.026	2.388	3.080	2.288	3.194	2.356	2.955	2.209	2.977	2.192	2.980	3.339
	β (Bar)	8.284	5.716	3.911	4.413	3.749	4.591	3.229	4.029	3.931	4.537	3.753	4.595	3.692	3.752
C29-1	ε_{11} (με)	0	657.0	158.7	786.5	158.2	919.1	160.8	1054.8	172.5	1196.0	197.3	1277.0	189.2	356.7
	ε_{33} (με)	0	-167.5	-32.6	-209.0	-34.3	-251.5	-41.1	-300.6	-50.6	-355.5	-62.3	-393.8	-67.2	-34.6
	k_v (E-18m^2)	1.584	1.055	1.313	1.152	1.337	1.218	1.402	1.206	1.402	1.323	1.407	1.486	1.544	1.905
	β (Bar)	5.884	5.654	3.691	4.303	3.696	3.546	3.258	4.125	3.532	3.567	3.889	3.292	3.805	3.088
C29-2	ε_{11} (με)	0	779.5	193.6	891.7	165.5	1019.8	165.1	1196.4	207.1	1430.9	252.3	1534.1	278.6	85.0
	ε_{33} (με)	0	-176.5	-61.1	-259.2	-58.4	-302.4	-65.4	-364.9	-76.9	-467.3	-117.3	-495.3	-123.1	-62.0
	k_v (E-18m^2)	1.651	1.454	1.682	1.436	1.748	1.436	1.768	1.460	1.892	1.567	1.872	1.583	1.880	2.108
	β (Bar)	6.817	5.139	4.740	4.356	3.777	4.206	3.727	4.103	3.173	4.374	3.789	4.028	3.662	3.311
C19-1	ε_{11} (με)	0	968.2	218.4	1151.4	213.7	1357.2	219.7	1581.5	246.4	1792.3	270.2	1917.3	282.6	64.2
	ε_{33} (με)	0	-210.8	-37.9	-274.2	-52.7	-334.4	-67.3	-378.4	-63.8	-439.6	-72.5	-482.9	-85.4	-47.6
	k_v (E-18m^2)	0.755	0.964	1.277	0.956	1.212	0.935	1.255	0.942	1.253	1.006	1.308	1.093	1.338	1.492
	β (Bar)	17.816	6.509	4.460	5.641	4.574	5.526	4.107	5.562	4.112	4.872	3.633	4.722	3.840	3.612
C19-2	ε_{11} (με)	0	751.1	194.7	916.2	220.3	1098.5	245.1	1250.2	286.9	1423.2	342.5	1536.4	359.2	164.5
	ε_{33} (με)	0	-116.2	-15.2	-146.8	-14.2	-184.6	-6.0	-208.4	2.4	-236.3	-12.0	-257.2	-4.9	10.2
	k_v (E-18m^2)	1.059	0.963	1.129	0.990	1.029	0.914	1.105	0.908	1.128	0.854	1.066	0.887	1.071	1.214
	β (Bar)	5.417	4.493	4.027	4.304	5.627	5.116	4.460	5.032	4.216	6.102	4.558	5.127	4.331	3.924

For another specimen C29-1, its intrinsic gas permeability behaviours in a totally different way from specimen C19-1. At the first loading level of 50% ultimate strength, the intrinsic gas permeability is about 30 percent lower than the situation before loading, showing significant compaction and solidation of pores under the loading condition of about 50% of its ultimate strength. Beyond 50% ultimate strength, the intrinsic gas permeability always increases with the rising of loading, indicating the controlling factors of development and opening of micro-cracks.

For the other specimens, their intrinsic gas permeability behaviours in a similar way. When the loading stress is smaller than about 70% ultimate strength, intrinsic gas permeability decreases with respect to loading stress and strain. Moreover, the intrinsic gas permeability becomes larger when loading level is increased beyond 70\% ultimate strength. Except the specimen C39-1, the change of intrinsic gas permeability is relatively small in the range of [-15%, 30%] comparing to the case before loading action. From the above analysis, it can be concluded that the transition point of axial loading stress is about 70% of its ultimate strength, although it may vary.

In terms of loading strain, the intrinsic gas permeability behaviours in a similar way to loading stress. It is emphasized that the transition point of strain ratio beyond which the intrinsic gas permeability begin to increase varies in a wide range from 0.4 to 0.8 of much scatter. From this consideration, it is more reasonable to control the loading stress lower than about 70% ultimate strength to prevent obvious increase of intrinsic gas permeability.

(2) Klinkenberg coefficient

As the Klinkenberg coefficient β is closely linked to the pore/micro-crack size, it is obviously different from each other due to the distinct of their pore / micro-crack size distribution. Similar to the analysis of intrinsic gas permeability, relative Klinkenberg coefficient β_r is also introduced and defined as the ratio of Klinkenberg coefficient under compression β_c to that before loading β_0,

$$\beta_r = \beta_c / \beta_0 \tag{6}$$

To further understand the evolution of micro-structure of concrete material under different uni-axial loading levels, the relationship between relative Klinkenberg coefficient β_r and relative stress / strain ratio σ_r, ε_r is also plotted, as shown in Figure 3.

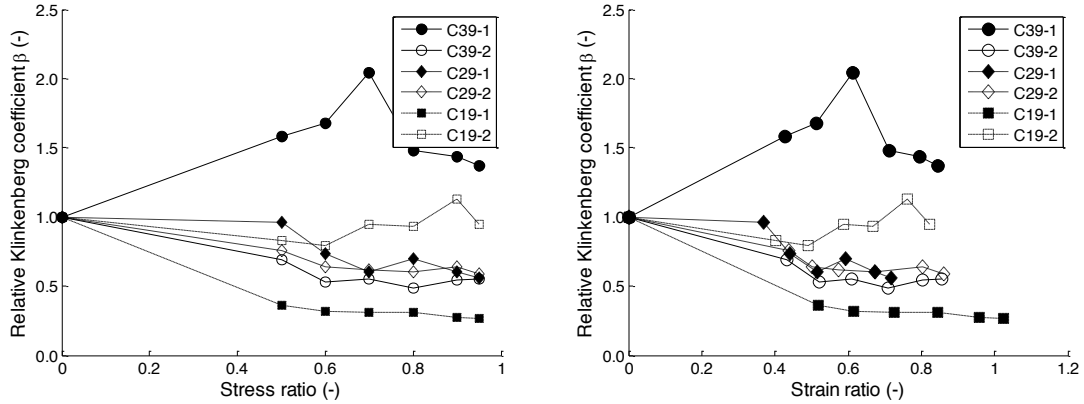

Figure 3 The evolution of relative Klinkenberg coefficient with stress ratio (Left) and strain ratio (Right).

From Figure 3, it is first observed that specimens C39-1, C19-1 and C 19-2 behave in special ways. It is well-known that Klinkenberg coefficient β is closely related to the mean size of pores and micro-cracks in certain sense, and it will increase if the mean size of pores and micro-cracks decreases. From this viewpoint, when concerning specimen C39-1, the mean size of pores and micro-cracks obviously decreases before 70% ultimate strength, which makes the intrinsic gas permeability significantly decreases. Beyond 70% ultimate strength, the mean size of pores and micro-cracks becomes larger with increasing loading stress. Correspondingly, the intrinsic gas permeability becomes larger. For another specimen C19-1, its Klinkenberg coefficient always decreases with respect to rising loading levels, meaning that the mean size of pores and micro-cracks monotonically increase but within a relative small degree. When concerning specimen C19-2, its mean size of pores and micro-cracks first slightly increases but then remarkably decrease if the loading stress is beyond 60% ultimate strength. For the other specimens, the Klinkenberg coefficient first quickly decrease with the rising loading level but then changes in a stable way with small variation. It can be further deduced that the pores and micro-cracks are first compacted obviously within about 60% ultimate strength. After that, the mean size of pores and micro-cracks are almost stable but the number of micro-cracks will be larger and larger, which makes their intrinsic permeability increase. The micro-structure of pores and micro-cracks (mean size, number, connectivity, opening) will be changed in a complex manner with respect to mechanical loading, which determines the evolution of intrinsic gas permeability.

Gas permeability after loading

After uni-axial loading with relative high stress, irreversible plastic strain will accumulate due to the nucleation and opening of micro-cracks. To distinguish the effect of accumulated plastic strain from elastic strain, the relationship between intrinsic gas permeability and plastic strains after loading are further analyzed. Since the lowest compressive stress 5 MPa applied in the loading history is very low, it is neglected and the corresponding strain is approximately thought to be identical to un-loading situation. Moreover, both the residual axial strain ε^r_{11} and volumetric strain $\varepsilon^r_V = \varepsilon^r_{11} + 2\varepsilon^r_{33}$. are analyzed with respect to the relative intrinsic gas permeability and Klinkenberg coefficient.

(1) Intrinsic gas permeability

Figure 4 shows the relationship between intrinsic gas permeability and residual axial / volumetric strains of much scatter. It can be inferred from the first sight that there is no clear relationships between them in terms of either residual axial strain or residual volumetric strain. For specimens C39-1 and C29-1, most of the permeability tested after loading is smaller than that tested before loading, meaning that the contribution of

micro-cracks to the permeability is less than the compaction of pores. For other specimens, the gas permeability is more or less larger than that measured before loading, which is more reasonable due to the micro-cracking or accumulated plastic strain. It is worthy noted that the increase of gas permeability for cracked specimens is limited by the relative high confining pressure (3MPa), which constraints the opening of micro-cracks.

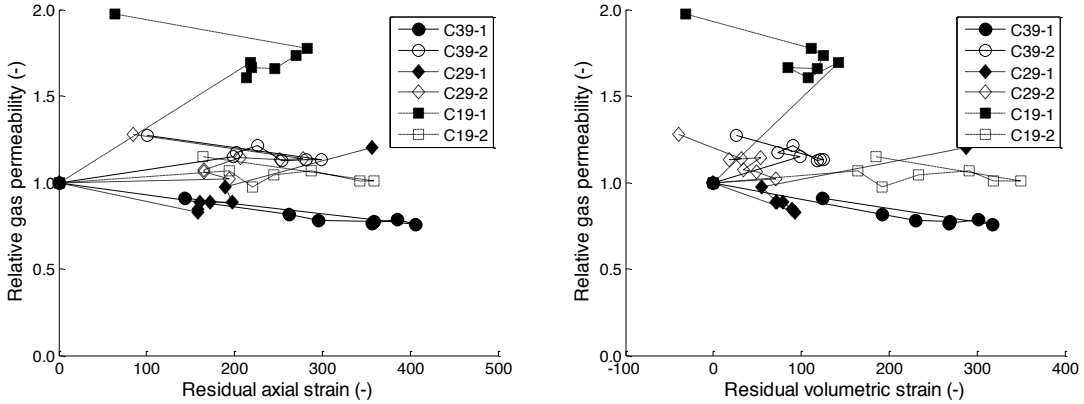

Figure 4 The evolution of relative intrinsic gas permeability with the residual axial strain (Left) and volumetric strain (Right).

(2) Klinkenberg coefficient

The relationships between relative Klinkenberg coefficient β_r and residual axial / volumetric strains are shown in Figure 5. Similar to the relationship between relative intrinsic gas permeability and the residual strains, there are no close links between relative Klinkenberg coefficient and both residual axial strain and relative volumetric strain. Except specimen C39-1, the Klinkenberg coefficient for other micro-cracked specimens are smaller than that measured before loading, indicating that the mean size of pores and micro-cracks are larger than original pores before loading. Since Klinkenberg coefficient represents the mean size of pores and micro-cracks and residual strain indicates the accumulation of micro-cracking, it is easily known from Figure 5 that the cracking pattern for both three structural concrete materials is remarkably complex and heterogeneous from the viewpoint of gas permeability.

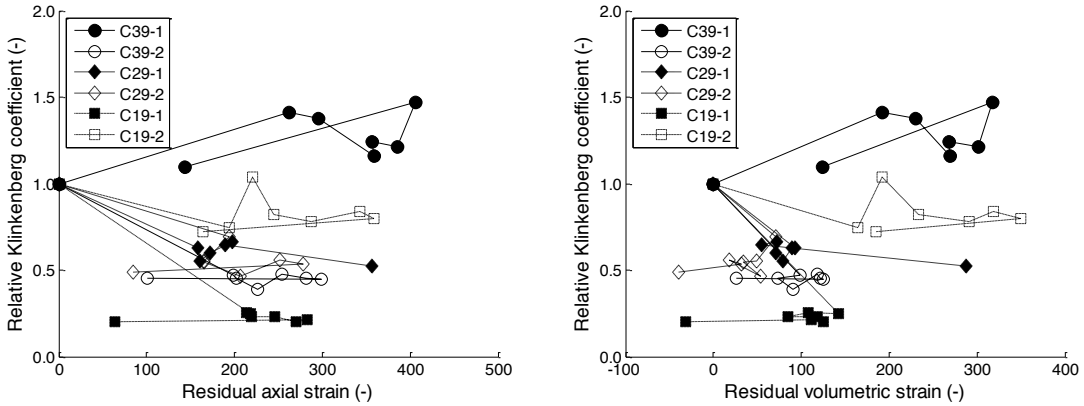

Figure 5 The evolution of relative Klinkenberg coefficient with the residual axial strain (Left) and volumetric strain (Right).

Relationship between gas permeability and Klinkenberg coefficient

Conceptually, both intrinsic gas permeability and Klinkenberg coefficient are determined by pores and micro-cracks of great complexity for concrete materials. Although gas permeability and Klinkenberg coefficient are not well correlated with macroscopic indicator of strains, there might be some links between them. Figure~\ref{fig-Kv-Beta} gives the relationship between intrinsic gas permeability and Klinkenberg coefficient for all situations of under or after loading in the loading history. Except only one points for specimen C19-2, other points follow a certain law. Inspired and borrowed from the suggested model explicitly giving the relationship between intrinsic gas permeability and Klinkenberg coefficient (Tanikawa and Shimamoto 2006;

Civan 2010), the relative Klinkenberg coefficient is approximated by the following formula in terms of relative intrinsic gas permeability as,

$$\beta_r = Bk_r^{-A} \tag{6}$$

in which A and B are constants. Through the least-square method, constant A and B is obtained as 1.60 and 0.65, respectively. And the fitting curve is also shown in Figure 6. It can be seen that this fitting curve can roughly capture the relationship between relative Klinkenberg coefficient and intrinsic gas permeability though the points are scattered.

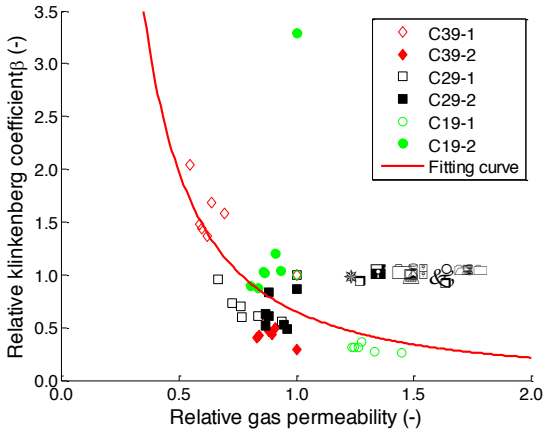

Figure 6 The relationship between relative intrinsic gas permeability and relative Klinkenberg coefficients.

CONCLUDING REMARKS

The evolution of gas permeability for three structural concrete materials are experimentally investigated under and after uni-axial loading. A highly developed permeater, which allows uni-axial loading, gas permeability and strain measurement at the same time, is employed to carry out this experimental research. The intrinsic gas permeability and Klinkenberg coefficient for totally dried cylinders are measured before, under and after a carefully designed loading history. The relationship between intrinsic gas permeability, Klinkenberg coefficient and uni-axial stress, elastic / plastic strains are thoroughly analysed. It is found that the transitional uni-axial stress beyond which the gas permeability begin to rise is about 70% ultimate strength. Under loading condition, the relationship between intrinsic gas permeability and elastic / plastic strains is not clear and much scatter always exist due to complex cracking pattern. In another aspect, the relationship between Klinkenberg coefficient and strains indicates that the mean size of pores and micro-cracks first increase and then keep almost stable under the action of confining pressure. While the number of micro-cracks obviously increases and makes the intrinsic gas permeability increasing. After loading, neither residual axial strain nor residual volumetric strain can characterize the evolution of intrinsic gas permeability and Klinkenberg coefficient. However, the relationship between intrinsic gas permeability and Klinkenberg coefficient can be approximately captured by a semi-empirical law, indicating the implied role of micro-cracks on both intrinsic gas permeability and Klinkenberg coefficient.

ACKNOWLEDGMENTS

The indispensable contribution of Prof. Frederic Skoczylas towards this experimental investigation and the financial supports from the National Natural Science Foundation of China (No. 51208153) for the current research are gratefully acknowledged.

REFERENCES

AFGC (French Association of Civil Engineering) (2007). “Concrete design for a given structure service life, State-of-the-art and guide for the implementation of a predictive performance approach based upon durability indicators”. AFGC Scientific and Technical Documents, Paris.

Benachour Y., Davy C., Skoczylas F., Houari H. (2008). “Effect of a high calcite filler addition upon microstructural, mechanical, shrinkage and transport properties of a mortar”. *Cement and Concrete Research* 38 (6), 727-736.

Cerny R., Rovnanikova P. (2002). “Transport processes in concrete”. Spon Press, London and New York.

Civan F. (2010). “Effective correlation of apparent gas permeability in tight porous media”. *Transport in Porous Media* 82(2), 375-384.

Davy, C. A., Skoczylas, F., Barnichon, J. D., Lebon, P. (2007). “Permeability of macro-cracked argillite under confinement: Gas and water testing”. *Physics and Chemistry of the Earth* 32 (8), 667–680

Hoseini, M., Bindiganavile, V., Banthia, N. (2009). “The effect of mechanical stress on permeability of concrete: A review”. *Cement and Concrete Composites* 31 (4), 213–220

Klinkenberg L. J. (1941). “The permeability of porous media to liquid and gas”. *Drilling and Production Practice*, 200-213.

Loosveldt, H., Lafhaj, Z., Skoczylas, F. (2002). “Experimental study of gas and liquid permeability of a mortar”. *Cement and Concrete Research* 32 (9), 1357–1363

Mehta, P. K., Monteiro, P. J. M. (2006). “Concrete: microstructure, properties and materials”. McGraw-Hill, New York.

Reinhardt, H. W. (1997). “Penetration and permeability of concrete: barriers to organic and contaminating liquids”, RILEM Report 16. E&FN Spon, London.

Scheidegger, A. E. (1974). “The physics of flow through porous media”. University of Toronto Press, Toronto.

Tanikawa,W., Shimamoto, T. (2006). “Klinkenberg effect for gas permeability and its comparison to water permeability for porous sedimentary rocks”. *Hydrology and Earth System Sciences Discussions* 3 (4), 1315–1338.

Verdier, J., Carcasses, M., Ollivier, J. P. (2002). “Modelling of a gas flow measurement — application to nuclear containment vessels”. *Cement and Concrete Research* 32 (8), 1331–1340.

Wang, W., Liu, J., Agostini, F., Davy, C., Skoczylas, F., Corvez, D. (2014). “Durability of an ultra high performance fiber reinforced concrete (UHPFRC) under progressive aging”. *Cement and Concrete Research* 55 (1), 1–13.

Wei, K. K., Morrow, N. R., Brower, K. R. (1986). “Effect of fluid, confining pressure, and temperature on absolute permeabilities of low-permeability sandstones”. *Society of Petroleum Engineers* 1 (4), 413–423.

Zhou, C., Li, K., Han, J. (2012a). “Characterizing the effect of compressive damage on transport properties of cracked concretes”. *Materials and Structures* 45 (3), 381–392.

Zhou, C., Li, K., Pang, X. (2012b). “Geometry of crack network and its impact on transport properties of concrete”. *Cement and Concrete Research* 42 (9), 1261–1272.